Title

Tet proteins influence the balance between neuroectodermal and mesodermal fate choice by inhibiting Wnt signaling

Journal

Proceedings of the National Academy of Sciences of the United States of America, 113(51)

ISSN

0027-8424

Authors

Li, Xiang
Yue, Xiaojing
Pastor, William A
et al.

Publication Date

2016-12-20

DOI

10.1073/pnas.1617802113

Peer reviewed

Tet proteins influence the balance between neuroectodermal and mesodermal fate choice by inhibiting Wnt signaling

Xiang Li[a,b], Xiaojing Yue[a], William A. Pastor[a,1], Lizhu Lin[c], Romain Georges[a], Lukas Chavez[a,2], Sylvia M. Evans[c,d,3], and Anjana Rao[a,b,e,f,3]

[a]Division of Signaling and Gene Expression, La Jolla Institute for Allergy and Immunology, La Jolla, CA 92037; [b]Sanford Consortium for Regenerative Medicine, La Jolla, CA 92037; [c]Skaggs School of Pharmacy and Pharmaceutical Sciences, University of California at San Diego, La Jolla, CA 92093; [d]Department of Medicine, University of California at San Diego, La Jolla, CA 92093; [e]Department of Pharmacology, University of California at San Diego, La Jolla, CA 92093; and [f]Moores Cancer Center, University of California at San Diego, La Jolla, CA 92093

Contributed by Anjana Rao, November 2, 2016 (sent for review October 14, 2016; reviewed by Kristin K. Baldwin and Scott J. Bultman)

TET-family dioxygenases catalyze conversion of 5-methylcytosine (5mC) to 5-hydroxymethylcytosine (5hmC) and oxidized methylcytosines in DNA. Here, we show that mouse embryonic stem cells (mESCs), either lacking Tet3 alone or with triple deficiency of Tet1/2/3, displayed impaired adoption of neural cell fate and concomitantly skewed toward cardiac mesodermal fate. Conversely, ectopic expression of Tet3 enhanced neural differentiation and limited cardiac mesoderm specification. Genome-wide analyses showed that Tet3 mediates cell-fate decisions by inhibiting Wnt signaling, partly through promoter demethylation and transcriptional activation of the Wnt inhibitor secreted frizzled-related protein 4 (*Sfrp4*). Tet1/2/3-deficient embryos (embryonic day 8.0–8.5) showed hyperactivated Wnt signaling, as well as aberrant differentiation of bipotent neuromesodermal progenitors (NMPs) into mesoderm at the expense of neuroectoderm. Our data demonstrate a key role for TET proteins in modulating Wnt signaling and establishing the proper balance between neural and mesodermal cell fate determination in mouse embryos and ESCs.

TET methylcytosine oxidases | mouse embryonic stem cells | Wnt signaling | DNA demethylation | neuromesodermal progenitors

TET (ten-eleven translocation) enzymes are a family of Fe(II) and 2-oxoglutarate–dependent dioxygenases, which successively oxidize 5-methylcytosine (5mC) to 5-hydroxymethylcytosine (5hmC), 5-formylcytosine (5fC), and 5-carboxylcytosine (5caC) in DNA (1–3). The three mammalian Tet proteins, Tet1, Tet2, and Tet3, possess homologous C-terminal catalytic domains as well as CXXC domains that bind unmodified CpGs (4), except that the CXXC domain of TET2 became separated from the catalytic domain during evolution and is now a separate protein known as IDAX/CXXC4 (5). The oxidized methylcytosine (oxi-mC) species generated by Tet enzymes facilitate DNA demethylation through both passive (replication-dependent) and active (replication-independent) mechanisms (4); they also function as epigenetic marks that bind transcription factors and chromatin-associated proteins, thereby influencing chromatin structure and gene expression (6–8).

Mice lacking individual TET proteins develop relatively normally until birth and beyond (9). Specifically, Tet1-deficient mice on a mixed 129/Sv × C57BL/6 background produce normal-sized litters (10), but display minor behavioral abnormalities and defects in learning, memory, and expression of neuronal activation-related genes (11, 12), as well as a tendency to develop B-cell lymphomas relatively late in life (13). Tet2-deficient mice on a pure C57BL/6 background are also viable and fertile; they exhibit mild hematopoietic phenotypes and occasionally develop myeloid malignancies late in life (14, 15). Tet3-deficient mice die perinatally for unknown reasons (16). Deletion of two of the three TET family members has more serious consequences. A significant fraction of mice lacking both Tet1 and Tet2 survive to adulthood, whereas the remaining pups succumb late in embryogenesis or shortly after birth (17). Embryos lacking Tet1 and Tet3 only survive to embryonic day 10.5 (E10.5) and display poor forebrain formation and abnormal facial structures (18). The 5hmC generated by Tet family dioxygenases is abundant in neurons (19) and may be critical for neural development (20). In *Xenopus*, Tet3 plays a vital function in early eye and neural development by directly targeting several key developmental genes (21). All of these studies indicate that TET-family proteins are involved in neural development, which prompted us to further study—through triple deletion of all three TET proteins—the in vivo functions and redundancy of TET proteins during neural development.

In vivo neurulation is a fundamental event of embryogenesis that culminates in the formation of the anterior neural plate (ANP) and the posterior neural plate (PNP), which are the precursors of the brain and spinal cord, respectively (22). The ANP is derived directly from the epiblast (23), whereas the development of the PNP from the epiblast involves an intermediate state of bipotent neuromesodermal progenitors (NMPs), which can give

Significance

Methylation of cytosine bases in DNA is an epigenetic modification that influences gene expression. TET (ten-eleven translocation)-family dioxygenases catalyze conversion of 5-methylcytosine (5mC) to 5-hydroxymethylcytosine (5hmC) and additional oxidized methylcytosines in DNA. Here, we show that both Tet3- and Tet1/2/3-deficient mouse ES cells showed impaired neural conversion, with skewing toward cardiac mesoderm. Genome-wide analyses showed that Tet3 mediates cell-fate decisions by inhibiting Wnt signaling. Consistent with these findings, Wnt signaling was hyperactivated in Tet1/2/3-deficient embryos, leading to aberrant differentiation of bipotent neuromesodermal progenitors into mesoderm at the expense of neuroectoderm. Our data demonstrate a key role for TET proteins in modulating Wnt signaling and establishing the proper balance between neural and mesoderm cell fate determination.

Author contributions: X.L., S.M.E., and A.R. designed research; X.L., X.Y., W.A.P., L.L., and R.G. performed research; X.L., X.Y., and L.C. analyzed data; and X.L., X.Y., S.M.E., and A.R. wrote the paper.

Reviewers: K.K.B., Scripps Research Institute; and S.J.B., University of North Carolina.

The authors declare no conflict of interest.

Data deposition: The sequences reported in this paper have been deposited in the Gene Expression Omnibus (GEO) database, www.ncbi.nlm.nih.gov/geo (accession nos. GSE89313, GSE89314, GSE89315, and GSE89316).

[1]Present address: Department of Molecular, Cell and Developmental Biology, University of California, Los Angeles, CA 90095.

[2]Present address: Division of Pediatric Neurooncology, German Cancer Research Center, 69120 Heidelberg, Germany.

[3]To whom correspondence may be addressed. Email: arao@lji.org or syevans@ucsd.edu.

This article contains supporting information online at www.pnas.org/lookup/suppl/doi:10.1073/pnas.1617802113/-/DCSupplemental.

rise to both the neurectoderm and mesoderm (24). Population fate maps at early somite stages have identified two regions containing NMPs: the dorsal layer of the node-streak border (NSB) and the caudal lateral epiblast (CLE) on either side of the primitive streak (PS) (24–27). In vitro, the induction of the neuroectoderm in ES cell (ESC) cultures is often referred to as the "default" pathway, because neuroectoderm readily develops in cultures that contain no serum or lack signaling through the Wnt, bone morphogenetic protein 4 (Bmp4), or activin signaling pathways (28–30).

Here we show that, in Tet3- and Tet1/2/3-deficient mouse ESCs (mESCs), differentiation of mESCs was skewed away from the default pathway of neuroectoderm lineage specification and toward the cardiac mesoderm fate. This phenotype appeared to be driven primarily by the absence of Tet3, because it was also observed in Tet3-deficient mESCs. Conversely, ectopic expression of Tet3 in mESCs promoted ectoderm differentiation and inhibited cardiac mesoderm differentiation. Through genome-wide chromatin immunoprecipitation-sequencing (ChIP-seq) and transcriptional profiling (RNA-sequencing; RNA-seq), we demonstrate that Tet3 mediates cell-fate decisions through inhibition of Wnt signaling, which was further corroborated by the fact that the skewed lineage specification in Tet3-deficient mESCs was rescued by treatment with Dickkopf1 (Dkk1), an extracellular inhibitor of Wnt signaling. Tet3-null mESCs showed decreased expression of genes encoding the Wnt signaling inhibitor secreted frizzled-related protein 4 (*Sfrp4*), correlating with increased DNA cytosine modification of the *Sfrp4* promoter. Consistent with mESC findings, Wnt signaling was hyperactivated in Tet1/2/3-deficient embryos, as evidenced by increased levels of activated β-catenin, leading to aberrant differentiation of bipotent NMPs into mesodermal lineages at the expense of neural lineages. In summary, our data demonstrate a key role for TET proteins in modulating Wnt signaling and establishing the proper balance between neural and mesodermal cell fate specification in mouse embryos and ESCs.

Results

Tet3 Regulates the Balance Between Neuroectoderm and Cardiac Mesoderm Differentiation in mESCs. To investigate the role of Tet3 during neuroectoderm differentiation, we used an efficient system for in vitro neural differentiation of mESCs: serum-free floating cultures of embryoid-body like aggregates, referred to as "SFEB" (29, 31). In SFEB cultures, mESCs undergo neuroectoderm differentiation by default, without the induction of mesodermal and endodermal differentiation (29, 31). Consistent with our previous observation during retinoic acid-induced mESC differentiation (32), the expression levels of *Tet1–3* displayed distinct patterns upon neural differentiation: *Tet1* mRNA declined rapidly; *Tet2* mRNA was initially maintained at a relatively steady level, then decreased on day 4, but recovered on day 6; and *Tet3* mRNA showed a progressive increase, with >40-fold up-regulation on day 6 of SFEB culture compared with the starting mESCs (Fig. 1*A*). This increase in *Tet3* transcripts was markedly reduced when the cultures were supplemented with inhibitory signals such as Bmp4 or FBS, both known to counteract neuroectoderm differentiation (28) (Fig. 1*B*). A similar pattern of *Tet1–3* expression was observed in whole embryos during embryogenesis in vivo (Fig. S1*A*). RNA-seq analysis of early embryos at E6.75 and E7.5 further corroborated the quantitative PCR (qPCR) results, showing that Tet1 and Tet2 expression decreased, whereas Tet3 expression increased, upon development in vivo (Fig. S1*B*). Whole-mount in situ hybridization analysis of early embryos at E9.25 showed substantial Tet3 expression in the brain and optic vesicle (Fig. 1*C*). These expression patterns of Tet3 in vitro and in vivo suggested that Tet3 might have a role in neuroectoderm differentiation.

To examine whether Tet3 is required for neuroectoderm differentiation in mESCs, we established a *Tet3*-deficient mESC line by Cre-mediated excision of exon 2 (Fig. S1*C*). mRNA levels of *Tet1* and *Tet2* were not altered, whereas *Tet3* mRNA was almost undetectable, in *Tet3* KO (*Tet3*$^{-/-}$) mESCs (Fig. S1*D*). When WT and *Tet3* KO mESCs were differentiated into embryoid bodies under serum-free conditions [SFEB (31)], neural marker genes *Sox1* and *Foxg1* showed a significant decrease at day 6, and the decrease was further enhanced at day 10 (Fig. 1*D*); moreover, mRNA expression levels of the cardiac precursor marker gene *Nkx2–5* and the mature cardiomyocyte marker genes *Myh6* and *Myh7* (encoding cardiac myosin heavy chains) and *Tnnt2* (encoding cardiac troponin T2; cTnT) increased dramatically in *Tet3* KO mESCs (Fig. 1*E*). The skewed gene expression pattern of *Tet3* KO cells was further corroborated at the protein level by immunostaining: A large portion of *Tet3* KO cells were cTnT^{+} under conditions where the majority of WT mESCs had undergone neural differentiation, as judged by Sox1 expression (Fig. 1*F*). Collectively, in the absence of Tet3, the default tendency of mESCs to differentiate toward neuroectoderm was skewed toward cardiac mesoderm differentiation.

Conversely, we carried out gain-of-function experiments by stably overexpressing Tet3 in mESCs. To test the effects of Tet3 overexpression on mESC differentiation, we used culture medium containing FBS, which promotes differentiation toward mesoderm rather than neuroectoderm (30). Ectopic expression of Tet3 induced substantial expression of the ectoderm marker gene *Fgf5* (Fig. 1*G*) and repressed expression of the cardiac lineage marker genes *Nkx2–5*, *Myh6*, *Myh7*, and *Tnnt2* (Fig. 1*H*), consistent with our observations of increased cardiac skewing in *Tet3* KO mESCs under serum-free (SFEB) culture conditions (Fig. 1*E*). This effect required the catalytic activity of Tet3, because expression of a catalytically inactive (HxD) mutant of Tet3, containing the amino acid substitutions H950D and Y952A (5) (Fig. S1*E*), did not alter *Fgf5* or cardiac mesoderm marker gene expression (Fig. 1 *G* and *H*). Collectively, these findings demonstrate that Tet3 functions as a key determinant of the selective differentiation of mESCs toward the neuroectoderm vs. the cardiac mesoderm cell fate, in a manner dependent on Tet3 catalytic activity.

Tet3-Dependent Transcriptional Programs During mESC Differentiation. To determine the effects of Tet3 gain and loss on global gene-expression profiles during mESC differentiation, we performed whole-transcriptome RNA-seq analysis of (*i*) WT and *Tet3* KO mESCs differentiating into neuroectoderm under SFEB culture conditions (days 6 and 10); and (*ii*) control and *Tet3*-expressing mESCs in nonpermissive neural differentiation conditions containing FBS (days 4 and 7). We defined 940 "Tet3-activated genes" that showed twofold or greater increase in expression in *Tet3*-expressing cells on day 4 or 7 and also twofold or greater decrease in expression in *Tet3* KO cells on day 6 or 10; similarly, we defined 1,355 "Tet3-repressed genes" that showed twofold or greater decrease in expression in Tet3-expressing cells on day 4 or 7, and also a twofold or greater increase in expression in *Tet3* KO cells on day 6 or 10 (Dataset S1). Gene Ontology (GO) analysis of Tet3-activated genes revealed a strong enrichment in functional categories relevant to neural developmental processes, including neuronal differentiation and brain development (Fig. 2*A*); conversely, Tet3-repressed genes were significantly implicated in mesoderm differentiation, including the skeletal system, vasculature, and heart development (Fig. 2*B*). Based on GO terms, we identified 46 Tet3-activated neural genes and 127 Tet3-repressed mesoderm genes (Fig. S2*A* and Dataset S1). To determine whether Tet3 directs neural differentiation by affecting extrinsic signaling pathways, we performed Ingenuity pathway analysis on genes differentially expressed in WT or *Tet3* KO mESCs on days 6 and 10 of SFEB culture. For all time points analyzed, differentially expressed genes were highly enriched in components of Wnt/β-catenin pathways (Fig. S2 *B* and *C*).

To determine the global distribution of Tet3 DNA occupancy, we performed ChIP coupled to high-throughput sequencing

(ChIP-seq) in neural precursor cells (NPCs). We chose to use NPCs for the ChIP-seq experiments because these cells display high expression of endogenous Tet3 (Fig. 1*A*) and constitute the endpoint of mESC differentiation under SFEB conditions (31). We identified 6,121 Tet3-bound regions (ChIP-seq peaks) in NPCs (Dataset S2), most of which were enriched in gene bodies and their immediate vicinity: By comparison with the mm9 reference genome, Tet3-binding sites were enriched in promoters and exons and to some extent also in 5′ and 3′ untranslated regions (UTRs), whereas peaks mapping to distal intergenic regions were substantially underrepresented (Fig. 2*C* and Fig. S2 *D* and *E*). Tet3-binding sites clustered close to transcription start sites (TSSs), with a low frequency of binding at distal regions relative to the TSSs (Fig. 2*D*), consistent with a previous report in which Tet3 binding regions were defined by pulldown with a GST fusion of the Tet3 CXXC domain (21). DNA motif analysis identified a CpG-rich sequence as the highest-ranked motif among Tet3-binding sites (Fig. 2*E*), also consistent with the previous report (21).

Validating the results of our RNA-seq data, GO analysis of Tet3 target genes (based on the presence of a Tet3 ChIP-seq peak within 10 kb of the TSS) showed enrichment for genes related to mesoderm development and neural differentiation (Fig. 2*F*). Ingenuity pathway analysis showed that Tet3 target genes were also strongly enriched for components of the Wnt signaling pathway (Fig. 2*G*), with the Notch signaling pathway being the second most highly enriched.

Tet3 Regulates mESC Differentiation via Modulation of the Wnt Signaling Pathway. To further investigate the relation between Tet3 and the Wnt signaling pathway, we assessed the effects of Tet3 on β-catenin/TCF-mediated transcription using the TOP-Flash luciferase reporter, which contains a minimal promoter adjacent to seven tandem TCF-binding sites; the FOP-Flash luciferase

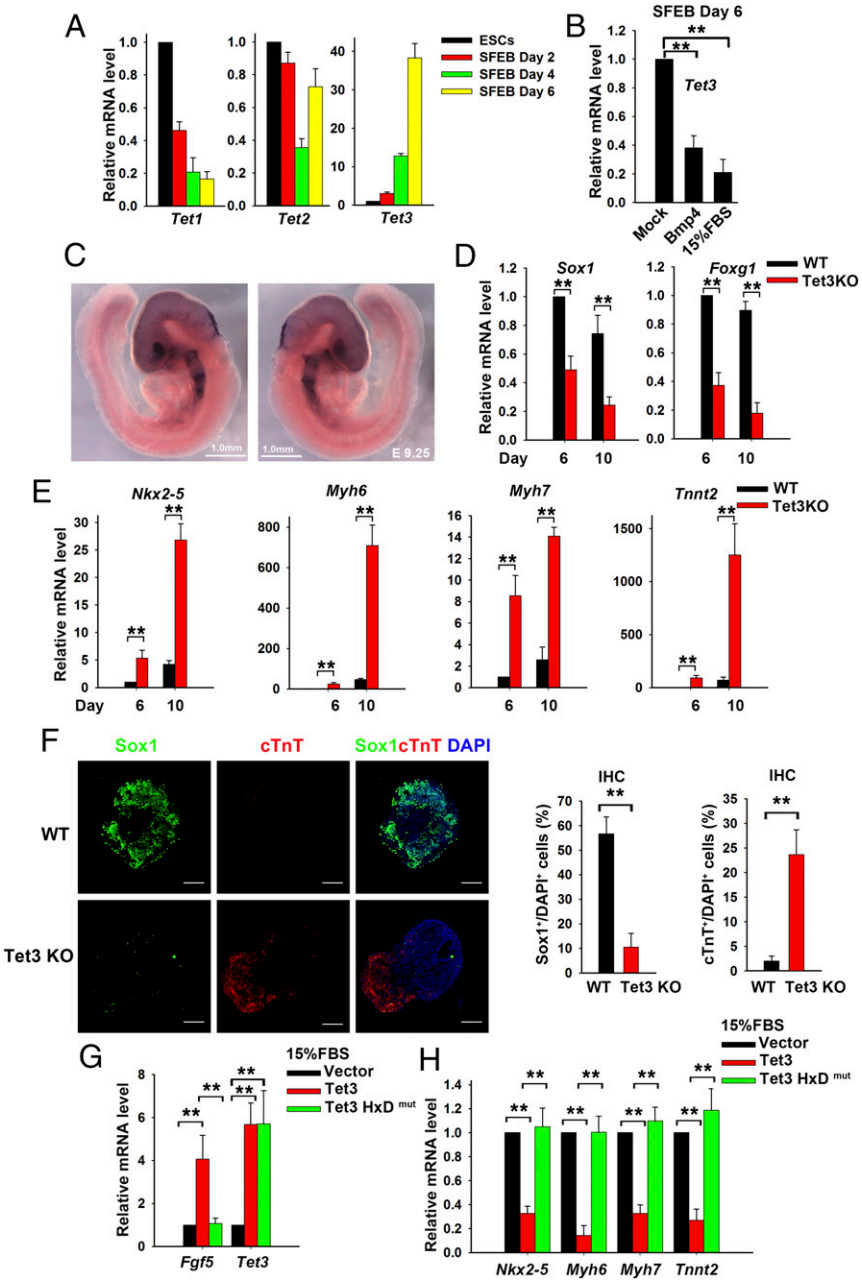

Fig. 1. Tet3 mediates neuroectoderm and cardiac mesoderm cell fate determination in mESCs. (*A*) Quantitative real-time PCR (qRT-PCR) analysis of *Tet1*, *Tet2*, and *Tet3* transcript levels in mESCs and neural cells differentiated by the SFEB method and normalized to the expression levels in mESCs (set at 1). Data are shown as mean ± SD (n = 3). (*B*) *Tet3* expression level in mESCs cultured in differentiation medium alone or in the presence of 10 ng/mL BMP4 or 15% (vol/vol) FBS. Data are shown as mean ± SD (n = 3). (*C*) Whole-mount in situ hybridization for *Tet3* mRNA at E9.25. (*D* and *E*) qRT-PCR analysis of transcripts of neural marker genes *Sox1* and *Foxg1* (*D*) and cardiomyocyte marker genes *Nkx2-5*, *Myh6*, *Myh7*, and *Tnnt2* (*E*). WT or *Tet3* KO mESCs were differentiated under SFEB culture conditions for 6 or 10 d. Data are shown as mean ± SD (n = 3). (*F*, *Left*) Immunocytochemistry of WT or *Tet3* KO mESCs differentiated under SFEB culture conditions for 10 d. Cells were stained with anti-Sox1 (green, neural cell marker) and anti-cTnT (red, cardiac cell marker) antibodies. Nucleus staining: DAPI (blue). (Scale bars: 100 μm.) (*F*, *Right*) Percentage of Sox1$^+$ or cTnT$^+$ cells in the total cell population. IHC, immunohistochemistry. (*G* and *H*) qRT-PCR analysis of transcripts of *Tet3* and ectoderm (*Fgf5*; *G*) or cardiomyocyte (*Nkx2-5*, *Myh6*, *Myh7*, and *Tnnt2*; *H*) marker genes in mESCs transfected with empty vector or vectors encoding Tet3 or Tet3HxD^{mut}. The cells were cultured in differentiation medium containing 15% (vol/vol) FBS for 7 d. Data are shown as mean ± SD (n = 3). $^{**}P < 0.01$.

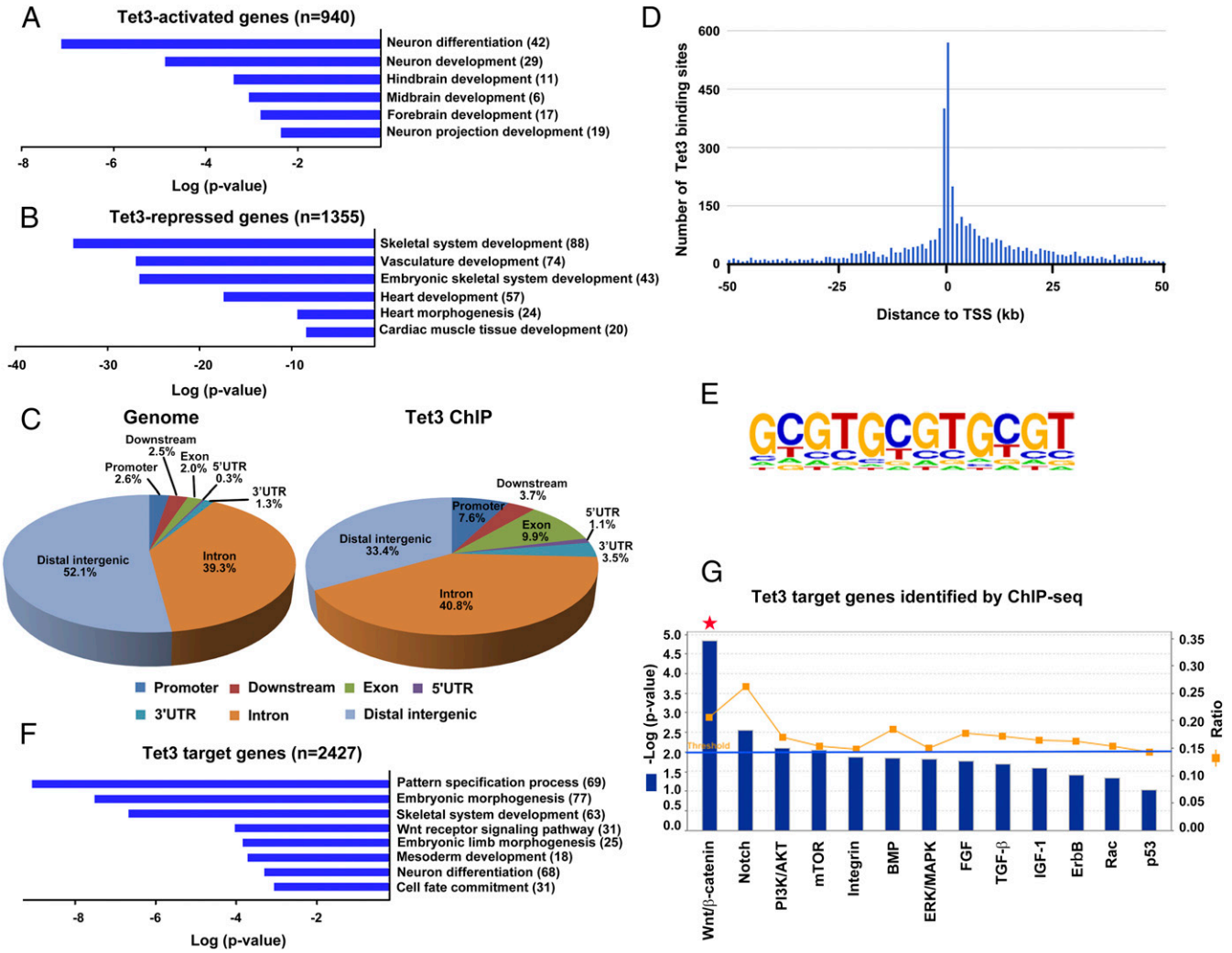

Fig. 2. Tet3-dependent transcriptional programs during mESC differentiation. (*A*) GO biological process analysis of Tet3-activated genes (defined as genes with twofold or greater increase in *Tet3*-overexpressing cells at day 4 or 7, concomitantly with twofold or greater decrease in *Tet3* KO cells at day 6 or 10, relative to WT control cells). (*B*) GO biological process analysis of Tet3-repressed genes (defined as genes with twofold or greater decrease in *Tet3*-overexpressing cells at day 4 or 7, concomitantly with twofold or greater increase in *Tet3* KO cells at day 6 or 10, relative to WT control cells). (*C*) Genomic distribution of Tet3-binding sites relative to their nearest RefSeq genes using the *cis*-regulatory element annotation system. "Promoter" was defined as 3 kb upstream from the TSS. "Downstream" was defined as 3 kb downstream from the 3′ end of the gene. "Distal intergenic region" refers to all locations outside the boundaries of a gene and the 3-kb region flanking the gene on either end. (*D*) Histogram showing the distribution of Tet3 ChIP-seq peaks relative to the nearest TSS. The majority of sites occupied by Tet3 in the genome are near the TSS (within ∼10 kb 5′ of the TSS and ∼25 kb 3′ of the TSS). (*E*) The highest-ranked DNA motif conserved in Tet3-bound loci revealed by de novo motif discovery analysis. (*F*) GO biological process analysis of Tet3 target genes (with at least one Tet3 ChIP-seq peak within 10 kb flanking the TSS). (*G*) Signaling pathway analysis (using Ingenuity Pathway Analysis software) of Tet3 target genes, defined as possessing a Tet3 ChIP-seq peak within the 10 kb flanking the TSS. The statistically significant canonical pathways are listed according to their *P* values (–Log10) (blue bars) and the ratio of Tet3 target genes found in each pathway over the total number of genes in that pathway (ratio) is shown by orange squares. The threshold line corresponds to a *P* value of 0.01. Note the predominance of genes in the Wnt/β-catenin signaling pathway among Tet3 target genes.

reporter, which contains mutated TCF binding sites, was used as a negative control (33). The activity of the β-catenin/TCF reporter decreased to 20% of control levels in Tet3-expressing cells (Fig. 3*A*), whereas it increased by almost twofold in *Tet3* KO cells relative to WT cells (Fig. 3*B*); again, expression of the catalytically inactive form of Tet3 (Tet3 HxD mutant) had no effect on reporter activity (Fig. 3*A*). These data suggest that Tet3 normally inhibits the Wnt/β-catenin signaling pathway and that the skewed differentiation observed in *Tet3* KO mESCs could be due to defective repression of the Wnt/β-catenin signaling pathway in the absence of Tet3.

To test this hypothesis, we used a well-known negative regulator of Wnt signaling—Dkk1, a secreted protein that acts extracellularly to inhibit Wnt-receptor interactions (34). Addition of Dkk1 to SFEB cultures reversed the skewed differentiation of *Tet3* KO mESCs away from neuroectoderm and toward cardiac mesoderm, as indicated by restored expression of the neural marker genes *Sox1* and *Foxg1* (Fig. 3*C*), and inhibited up-regulation of the cardiac mesoderm marker genes *Nkx2-5*, *Myh6*, *Myh7*, and *Tnnt2* (Fig. 3*D*). Whole-transcriptome RNA-seq analysis revealed that the expression of 30 of 46 Tet3-related neural genes was restored, and the expression of 110 of 127 Tet3-related mesoderm genes was repressed, in *Tet3* KO mESCs of SFEB culture in the presence of Dkk1 (Fig. S3 and Dataset S1). Collectively, these functional data combined with our genome-wide transcriptional and ChIP-seq data suggest that Tet3 regulates mESC differentiation by repressing Wnt signaling to regulate neuroectoderm vs. cardiac mesoderm cell fate.

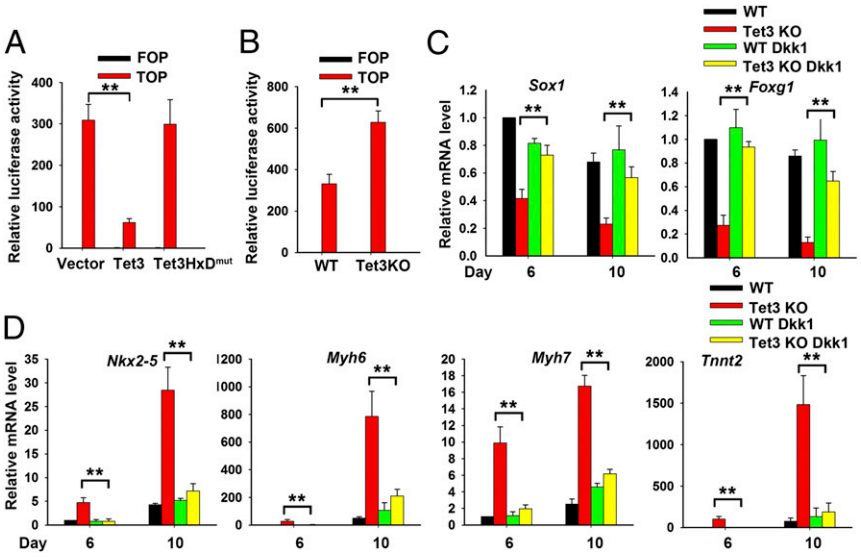

Fig. 3. Tet3 regulates mESC differentiation by modulating Wnt/β-catenin signaling. (*A* and *B*) TOP/FOP-Flash luciferase reporter assay in vector, Tet3, or Tet3-HxD^{mut} transduced mESCs (*A*) and in WT and *Tet3* KO mESCs (*B*) induced to differentiate by withdrawal of LIF plus addition of 0.1 μM *all-trans* retinoic acid (RA) for 4 d. Data are shown as mean ± SD ($n = 3$). (*C* and *D*) qRT-PCR analysis of transcripts of neural marker genes *Sox1* and *Foxg1* (*C*) and cardiomyocyte marker genes *Nkx2-5*, *Myh6*, *Myh7*, and *Tnnt2* (*D*). WT and *Tet3* KO mESCs were differentiated under SFEB culture conditions for 6 or 10 d in the absence or presence of the Wnt inhibitor Dkk1 (100 ng/mL). Data are shown as mean ± SD ($n = 3$). $^{**}P < 0.01$.

Tet3 Influences the Expression and DNA Modification Status of the Wnt Inhibitor *Sfrp4*. Combining our RNA- and ChIP-seq data, we identified 19 Tet3 target genes related to the Wnt/β-catenin signaling pathway (Dataset S1). Of these, the gene encoding *Sfrp4* drew our attention: *Sfrp4* possesses a domain similar to one in the Wnt receptor Frizzled protein and therefore can act as an inhibitor of Wnt signaling by preventing Wnt receptor binding: Epigenetic inactivation of the *Sfrp4* gene results in constitutive Wnt/β-catenin signaling (35, 36). In ChIP-seq assays, Tet3 directly bound the promoter region of *Sfrp4* in NPCs (Fig. 4*A*); moreover, *Sfrp4* mRNA expression was dramatically down-regulated in *Tet3* KO mESCs on day 6 of SFEB culture relative to WT control cells (Fig. 4*B*), whereas ectopic Tet3 expression induced substantial expression of *Sfrp4*, an effect that depended on the catalytic activity of Tet3 based on the fact that catalytically inactive (HxD mutant) Tet3 had no effect (Fig. 4*C*). Finally, stable expression of *Sfrp4* in differentiating mESCs mimicked the effect of ectopic Tet3 expression: In luciferase assays using the β-catenin/TCF reporter, Wnt activity was inhibited (Fig. 4*D*), and there was substantial induction of the ectoderm marker gene *Fgf5* (Fig. 4*E*) and repression of the cardiac lineage marker genes *Nkx2-5*, *Myh6*, *Myh7*, and *Tnnt2* (Fig. 4*F*).

It is known that *Sfrp4* expression is highly correlated to the methylation status of its promoter region (36). To investigate the relation of *Sfrp4* expression to Tet3 function and changes in DNA methylation, we performed bisulfite-sequencing (BS-seq) to examine whether the down-regulation of *Sfrp4* transcripts in differentiating *Tet3* KO cells correlated with alterations of DNA cytosine modification. Because BS-seq cannot distinguish 5mC and 5hmC (37), cytosines not deaminated by bisulfite treatment are designated "5mC+5hmC." In *Tet3* KO mESCs on day 6 of SFEB culture, the percentage of "5mC+5hmC" in the promoter region of *Sfrp4* increased compared with WT control cells across all of the CpGs analyzed (Fig. 4*G*). Together, these data suggest that Tet3 directly binds to and alters the DNA modification status of the *Sfrp4* locus and regulates *Sfrp4* transcription; in turn, Sfrp4 expression results in decreased Wnt signaling.

In addition to *Sfrp4*, our ChIP-seq data also showed that Tet3 directly bound each promoter region of a gene cluster encoding the protocadherin-alpha cluster (*Pcdha*) in NPCs (Fig. S4*A*). The *Pcdha* cluster contains 14 variable exons, each regulated by its own promoter, followed by three constant exons, and is highly expressed in neurons (38). Except for *Pcdha8* and *Pcdhac2*, expression of all genes in the *Pcdha* cluster was dramatically down-regulated in *Tet3* KO mESCs on day 6 of SFEB culture relative to WT control cells (Fig. S4*B*). The transcription of specific *Pcdha* isoforms has been shown to correlate significantly with the methylation status of the promoter and 5′ region of the first exon (39). In *Tet3* KO mESCs on day 6 of SFEB culture, the percentage of 5mC+5hmC in the promoter regions of *Pcdha4*, *Pcdha9*, *Pcdha12*, and *Pcdhac1* increased compared with WT control cells across the majority of CpGs analyzed (Fig. S4 *C*–*F*), whereas the methylation status of the promoter regions of *Pcdha8* and *Pcdhac2*—the two isoforms whose mRNA expression was unaltered—remained unchanged (Fig. S4 *G* and *H*).

It has been reported that the Pcdh superfamily functions to inhibit Wnt signaling (40–42). However, in our hands, transient expression of *Pcdha4* and *Pcdha7* during mESC differentiation inhibited Wnt signaling activity only moderately, based on a β-catenin/TCF reporter assay (less than twofold; Fig. S4*I*). Thus, Tet3 regulates the expression levels and the DNA modification status of the promoter regions of *Sfrp4* and certain genes of the *Pcdha* cluster, and at least part of the ability of Tet3 to diminish Wnt signaling may be mediated through increased Tet3-mediated expression of Sfrp4. Given the lack of an embryonic phenotype in Sfrp4-deficient mice (43), additional factors likely contribute to the increased Wnt signaling activity in *Tet3* KO cells.

Phenotype of Tet3-Deficient mESCs Is Exacerbated by Concurrent Deficiency of Tet1 and Tet2. The data from *Tet3* KO mESCs prompted us to look for developmental abnormalities in Tet3-deficient mice. As reported for 129Sv-background *Tet3* KO mice (16), the C57BL/6-background Tet3-deficient pups generated in our laboratory survived until birth, but all pups showed perinatal lethality. Phase-contrast images of E18.5 embryos and hearts from WT and *Tet3* KO mice showed no obvious developmental abnormalities of cardiac or other tissues. Nevertheless, qPCR and immunostaining analysis of the whole hearts from WT and *Tet3* KO embryos (E18.5) showed an increase of the cardiac progenitor marker Isl-1, a target gene of Wnt/β-catenin signaling (44) in the *Tet3* KO heart, especially in the right ventricle (Fig. S5). Thus, deficiency of Tet3 alone does not severely block embryonic development in vivo.

We hypothesized that the lack of overt cardiac and neuronal phenotypes in Tet3-deficient mice was most likely due to functional redundancy from the other two Tet family members, Tet1 and Tet2. To investigate this potential redundancy between Tet proteins, we generated *Tet1/2/3 fl/fl* mice from mice bearing the individual floxed alleles (14, 18) and used them to generate *Tet1/2/3 fl/fl* mESCs. These were then transiently transfected with a Cre expression plasmid to establish a Tet1/2/3 triple-deficient mESC

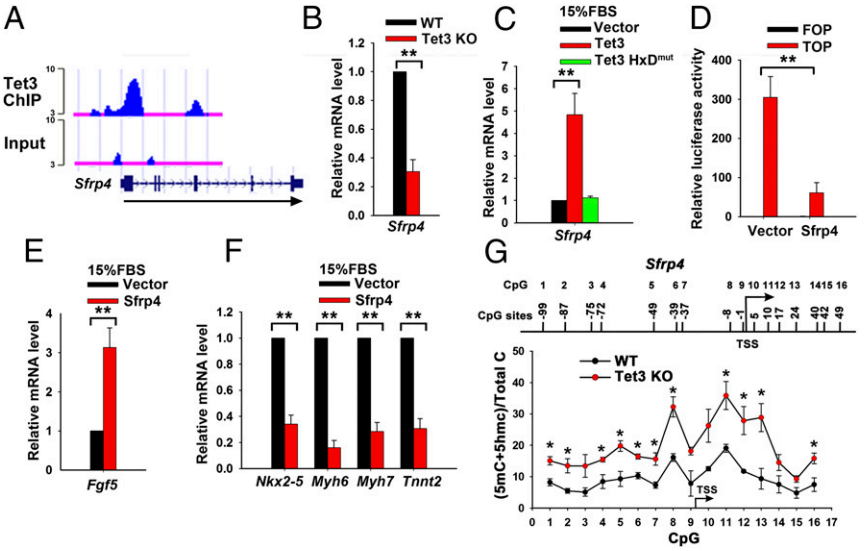

Fig. 4. Tet3 regulates mESC differentiation through Sfrp4, an inhibitor of the Wnt signaling pathway. (*A*) University of California Santa Cruz Genome Browser snapshots showing Tet3 ChIP-seq peaks at the TSS and in the gene body of *Sfrp4*. The exon–intron structure of the *Sfrp4* gene is shown below. The arrow shows the direction of transcription. The *y* axis of binding profiles denotes numbers of sequence tag reads. (*B*) qRT-PCR analysis of *Sfrp4* transcripts in WT and *Tet3* KO mESCs on day 6 of SFEB culture. Data are shown as mean ± SD ($n = 3$). (*C*) qRT-PCR analysis of *Sfrp4* transcripts. Vector-, Tet3-, or Tet3HxD^{mut}-transduced mESCs were cultured in differentiation medium containing 15% (vol/vol) FBS for 7 d. Data are shown as mean ± SD ($n = 3$). (*D*) TOP/FOP-Flash luciferase reporter assay in vector and Sfrp4-transduced mESCs induced to differentiate by withdrawal of LIF plus addition of 0.1 μM *all-trans* retinoic acid for 4 d. Data are shown as mean ± SD ($n = 3$). (*E* and *F*) qRT-PCR analysis of transcripts of ectoderm marker gene *Fgf5* (*E*) and cardiomyocyte maker genes *Nkx2-5*, *Myh6*, *Myh7*, and *Tnnt2* (*F*). Vector or Sfrp4-transduced mESCs were cultured in differentiation medium containing 15% (vol/vol) FBS for 7 d. Data are shown as mean ± SD ($n = 3$). (*G*) Bisulfite sequencing showing the percentage of 5mC+5hmC at each CpG site in the promoter region of *Sfrp4* in WT and *Tet3* KO mESCs on day 6 of SFEB culture. The positions of CpG sites are indicated relative to the TSS. Data are shown as mean ± SD ($n = 2$). *$P < 0.05$; **$P < 0.01$.

line (*Tet1/2/3* TKO mESCs) in which *Tet1*, *Tet2*, and *Tet3* mRNAs were completely undetectable (Fig. S6*A*). The proliferation of these *Tet1/2/3* TKO mESCs was significantly slower compared with the WT controls (Fig. S6*B*). Consistent with a previous report (45), neuroectoderm and cardiac mesoderm markers were all decreased during differentiation of *Tet1/2/3* TKO mESCs in serum-containing cultures compared with the WT controls (Fig. S6 *C* and *D*).

We used medium supplemented with 10% (vol/vol) knockout serum replacement (KSR) medium to compare WT, *Tet3* KO, and *Tet1/2/3* TKO mESC differentiation in serum-free conditions; this culture condition was chosen because it supported *Tet1/2/3* TKO mESC survival and differentiation better than the conditions used for Fig. 1*D* (N2B27 media; *SI Materials and Methods*). At day 7 of SFEB culture in 10% (vol/vol) KSR, *Tet3* KO mESC showed a milder decrease of the neuroectodermal markers *Sox1 and Foxg1* relative to WT cells than in N2B27 medium (compare Fig. S6*E* with Fig.1*D*); they also showed a significant increase of the mesoderm marker *T* (*Brachyury*) and a mild increase of the cardiac precursor marker Nkx2–5, but no change in the expression of the mature cardiomyocyte markers *Myh7* and *Tnnt2* (Fig. S6*F*). In contrast, compared with *Tet3* KO cells, *Tet1/2/3* TKO cells showed a more significant decrease of the neuroectoderm marker genes *Sox1* and *Foxg1* (compare Fig. 5*A* with Fig. S6*E*) and a more dramatic increase of the cardiac precursor marker *Nkx2-5* and the mature cardiomyocyte markers *Myh7* and *Tnnt2* (compare Fig. 5*B* with Fig. S6*F*). Therefore, in 10% (vol/vol) KSR serum-free conditions, cell differentiation was skewed only toward early mesoderm in *Tet3* KO mESCs; however, it could go further toward the cardiac mesoderm stage in *Tet1/2/3* TKO ESCs. The previously mentioned *Tet3* target gene, *Sfrp4*, which encodes a Wnt inhibitor, was also decreased in *Tet1/2/3* TKO mESCs after differentiation under SFEB conditions (Fig. S6 *G* and *H*). In addition, we found that the expression level of another Pcdh superfamily member, Pcdh8, was decreased significantly in *Tet1/2/3* TKO mESCs after differentiation under SFEB conditions (Fig. S6*I*). In light of a previous report showing that Pcdh8 can inhibit Wnt signaling activity (42), it is possible that down-regulation of both Sfrp4 and Pcdh8 contribute to increasing Wnt signaling in *Tet1/2/3* TKO cells.

TET Proteins Control the Balanced Differentiation of Neuromesodermal Progenitors During Early Embryogenesis in Vivo. To examine phenotypes of embryos lacking all three TET proteins, we generated Tet1/2/3 triple-deficient progeny by crossing *Zp3*- and *Stra8-Cre* mice with *Tet1/2/3 fl/fl* mice to generate mice in which expression of all three Tet proteins was abrogated in oocytes and sperm respectively. The progeny of *Tet1/2/3 fl/fl Zp3-Cre* female and *Tet1/2/3 fl/fl Stra8-Cre* male (hereafter termed *Tet1/2/3* TKO or TKO mice/embryos) lack all three TET proteins beginning at the zygotic stage.

In *Tet1/2/3* TKO embryos at early streak stages (E6.75), most decidua (31 of 42) were empty, and no degenerating embryos were observed, which may be due to the defects in oocytes in the absence of Tet proteins. However, surviving embryos (11 of 42) were morphologically indistinguishable from controls (Fig. S7*A*). Single-embryo RNA-seq of control and *Tet1/2/3* TKO embryos (E6.75; four embryos from each group) showed efficient deletion of the targeted "floxed" exons (flanked by *LoxP* sites) of each Tet gene (Fig. S7*B*). GO analysis of the 69 genes whose expression levels were most significantly altered in *Tet1/2/3* TKO embryos relative to controls (Fig. S7*C* and Dataset S3) revealed that up-regulated genes were implicated in mesoderm formation, including skeletal system development and limb morphogenesis (Fig. S7*D*): Cardiac progenitor marker genes (*Gata4* and *Fgf10*) and genes related to embryonic limb and skeletal development (*Six1*, *Six4*, *Alx1*, *Alx3*, *Bin1*, *Hoxd13*, and *Crabp2*) were all significantly increased in *Tet1/2/3* TKO embryos compared with control embryos (Fig. 5*C* and Fig. S7*E*). In contrast, the neural initiator Neuronatin (*Nnat*), which acts as an intrinsic factor to promote neural fate in mammals and *Xenopus* (46), was decreased in *Tet1/2/3* TKO embryos (Fig. 5*C*). Thus, triple TET deficiency promotes expression of mesoderm-related genes during early embryogenesis in vivo.

At mid-/late-streak stages (E7.25–7.5), we observed a developmental delay in *Tet1/2/3* TKO embryos: When the control embryos were at late-streak stage, the *Tet1/2/3* TKO embryos appeared to be at the midstreak stage (Fig. S8*A*). However, *Tet1/2/3* TKO embryos at E7.5 were morphologically indistinguishable from control embryos at E7.25. Immunostaining results showed that in *Tet1/2/3* TKO embryos at E7.5, the neural marker Sox2 was expressed in neuroectoderm (Fig. S8 *B*, *Lower*), the T-box transcription factor T (Brachyury) was expressed in the PS (Fig. S8 *C*, *Lower*), whereas Sox2^{+}T^{+} NMPs, which give rise to both neuroectoderm and mesoderm, were detected in the PS close to the node (Fig. S8 *D*, *Lower*). These staining patterns were similar to those in WT control embryos at E7.25 (Fig. S8 *B*–*D*, *Upper*).

At head-fold stages (E8.0–8.25), clear morphological differences between WT and *Tet1/2/3* TKO embryos were observed

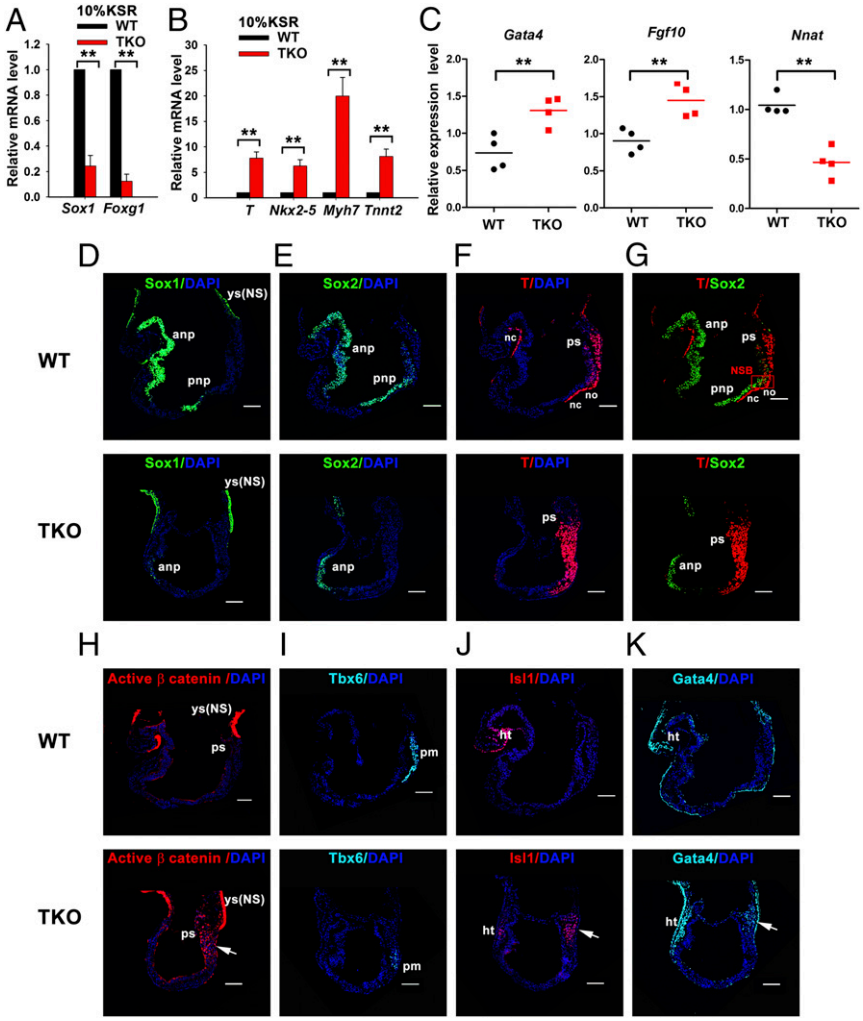

Fig. 5. TET proteins control the balanced differentiation of NMPs during early embryogenesis in vivo. (*A* and *B*) qRT-PCR analysis of transcripts of neural marker genes *Sox1* and *Foxg1* (*A*) and cardiac mesoderm marker *T* (*Brachyury*), *Nkx2-5*, *Myh7*, and *Tnnt2* (*B*). WT or *Tet1/2/3* KO (TKO) mESCs were differentiated under SFEB culture conditions for 7 d in 10% (vol/vol) KSR. Data are shown as mean ± SD ($n = 3$). (*C*) RNA-seq data for cardiac progenitor marker genes (*Gata4* and *Fgf10*) and neural initiator gene *Nnat* at E6.75 of WT and *Tet1/2/3* TKO embryos. (*D–K*) Immunocytochemistry of WT or *Tet1/2/3* TKO at E8.0–E8.25 for Sox1 (*D*), Sox2 (*E*), T (Brachyury) (*F*), Sox2 and T (*G*), active β-catenin (*H*), Tbx6 (*I*), Isl1 (*J*), and Gata4 (*K*). ht, heart; no, node; NS, nonspecific; pm, paraxial mesoderm; so, somites; yc, yolk sac. Nucleus staining: DAPI (blue). (Scale bars: 100 μm.) WT ($n = 3$); TKO ($n = 4$). $^{**}P < 0.01$.

(Fig. 5 *D–K*). To investigate the nature of these patterning defects, we analyzed expression of characteristic lineage markers by immunocytochemistry. In WT embryos, the primordial neural gene Sox1 was maintained throughout the ANP, which later differentiates into the brain, and the PNP; in contrast, in *Tet1/2/3* TKO embryos, Sox1 expression was significantly reduced (Fig. 5*D*). Note that in these figure panels, we observed nonspecific staining of the yolk sac [indicated by ys(NS)].

In WT embryos, strong expression of Sox2 was observed in ANP and PNP (Fig. 5*E*, *Upper*), whereas T (Brachyury) was expressed in the PS, ventral node (no), and notochord (NC) (Fig. 5*F*, *Upper*). Sox2 and T were coexpressed in the NSB, where the dual-fated NMPs are located. NMPs have the capacity to develop into body midline tissues—PNP, somites (so), and NC (Fig. 5*G*, *Upper*). However, in *Tet1/2/3* TKO embryos, Sox2 expression was only observed in ANP, and was completely absent in posterior regions of the embryos (Fig. 5*E*, *Lower*), whereas T (Brachyury) was readily detected in PS (Fig. 5*F*, *Lower*). Moreover, colocalization of Sox2 and T was not detected in the NSB region in *Tet1/2/3* TKO embryos (Fig. 5*G*, *Lower*).

Activation of Wnt signaling can prevent NMPs from adopting a neural cell fate, because high Wnt3a levels in PS down-regulate Sox2 expression (47). To examine whether Wnt activity was altered in *Tet1/2/3* TKO embryos, we analyzed expression of the active, dephosphorylated form of β-catenin. Immunostaining results showed that, in comparison with WT control embryos, there were strong signals for the active form of β-catenin in *Tet1/2/3* TKO embryos overlapping the T (Brachyury)-positive PS region at both midstreak (E7.25–7.5) and head-fold (E8.0–8.25) stages (Fig. 5*H* and Fig. S8*E*, arrow).

In WT embryos, NMPs give rise to both neuroectoderm and paraxial mesoderm, as indicated by immunostaining for the neural marker Sox2 and the paraxial mesoderm marker Tbx6 (Fig. 5 *E* and *I*, *Upper*). However, in *Tet1/2/3* TKO embryos, in addition to loss of Sox2 expression, expression of Tbx6 was significantly reduced (Fig. 5 *I*, *Lower*), suggesting an inability of NMPs to develop into paraxial mesoderm in *Tet1/2/3* TKO embryos. Next, we examined expression of lateral mesodermal markers Isl1 and Gata4. Anterior lateral mesoderm can give rise to cardiac mesoderm and further form the heart (48). We found that both Isl1 and Gata4 were ectopically coexpressed in the caudal region of *Tet1/2/3* TKO embryos,

in addition to their normal expression in the heart region (Fig. 5 *J* and *K*, *Lower*, arrow). In contrast, in WT control embryos at this stage, Isl1 and Gata4 were coexpressed only in the cardiogenic region (Fig. 5 *J* and *K*, *Upper*). The observation in *Tet1/2/3* TKO embryos of ectopic expression of cardiac mesodermal markers in the absence of neural plate is consistent with prior studies, which demonstrated that factors within neural plate signal to adjacent paraxial mesoderm to prevent its adopting a cardiac mesodermal fate (49). Thus, in *Tet1/2/3* TKO embryos, the absence of PNP would lead to a lack of repressive signals from neural plate, and therefore mutant NMPs, unable to form neuroectoderm, would adopt cardiac mesodermal rather than paraxial mesodermal cell fate.

At slightly later stages (E8.25–8.5), a striking feature of *Tet1/2/3* TKO embryos was the complete absence of neural plate, somite, and NC (Fig. 6 *A*–*H*). In *Tet1/2/3* TKO embryos, neural markers Sox1 and Sox2 were expressed in the ANP, but the territory of expression was reduced to varying extents (Fig. 6 *A* and *B, Lower*); T (Brachyury) was expressed in the PS at the caudal end of the embryo, where Wnt signaling was hyperactivated, as indicated by ectopic expression of active β-catenin (Fig. 6 *C* and *E, Lower*, arrow). We also observed that in *Tet1/2/3* TKO embryos, the paraxial mesoderm marker Tbx6 was again reduced in anterior PS (Fig. 6*F*, *Lower*), and the lateral mesoderm markers Gata4 and Isl1 continued to be ectopically expressed in the anterior PS region (Fig. 6 *G* and *H*, *Lower*, arrow). Because Gata4 and Isl1 can also mark endodermal tissues in the cardiogenic region, we examined expression of the endodermal marker Foxa2. Notably, cells ectopically expressing Gata4 and Isl1 were negative for the endoderm

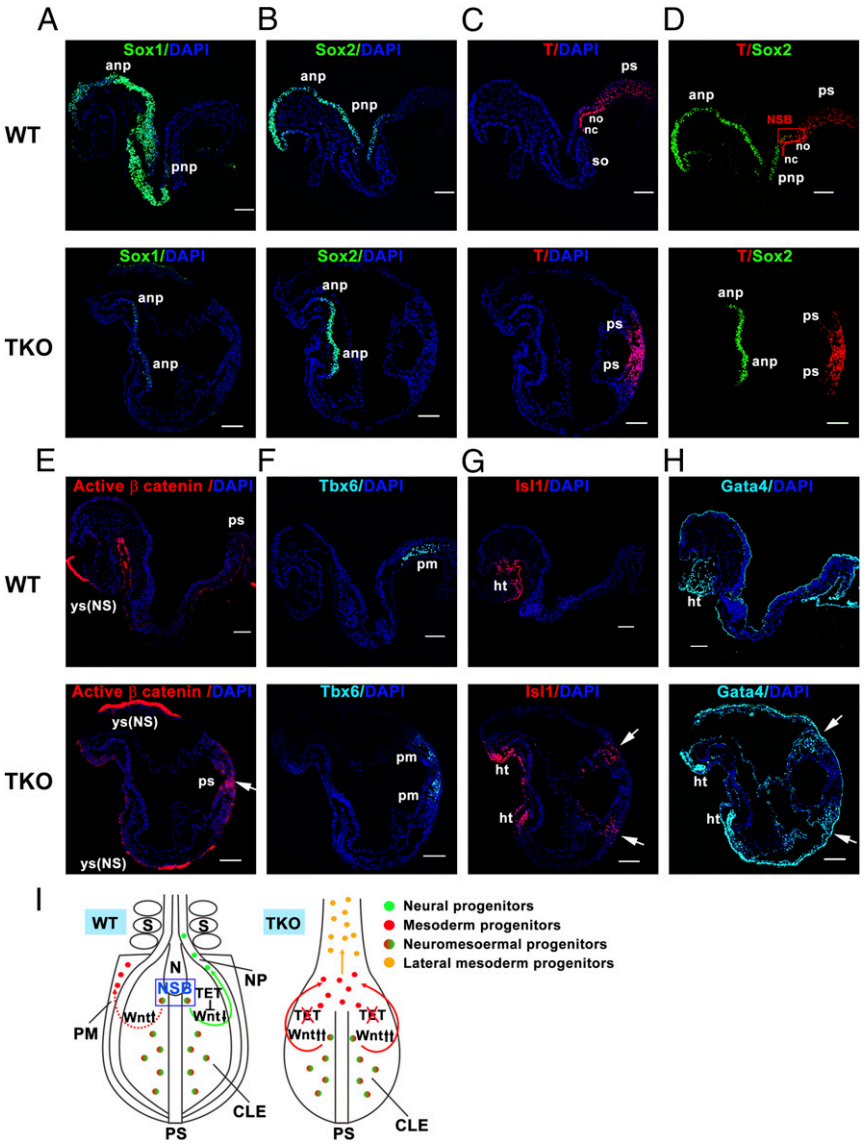

Fig. 6. Molecular analysis of *Tet1/2/3* TKO embryos at E8.25–8.5. (*A*–*H*) Immunocytochemistry of *Tet1/2/3* TKO at E8.25–8.5 for Sox1 (*A*), Sox2 (*B*), T (Brachyury) (*C*), Sox2 and T (*D*), active β-catenin (*E*), Tbx6 (*F*), Isl1 (*G*), and Gata4 (*H*). Due to the failure of neural plate closure, both left and right sides of the embryo are shown in *Tet1/2/3* TKO embryo sections. ht, heart; no, node; NS, nonspecific; pm, paraxial mesoderm; so, somites; yc, yolk sac. Nucleus staining: DAPI (blue). (Scale bars: 100 μm.) WT ($n = 3$); TKO ($n = 3$). (*I*) A model for TET function in developmental specification of NMPs in the E8.5 mouse embryo. In WT embryos, NMPs (red/green) are located in the NSB and CLE. When Wnt signaling is inhibited by Tet proteins, NMPs give rise to neural progenitors (green) which will contribute to the neural plate (NP), whereas activated Wnt signaling promotes the development of NMPs to mesoderm progenitors (red), which will contribute to paraxial mesoderm (PM). In *Tet1/2/3* TKO embryos, Wnt signaling is abnormally activated in the absence of TET proteins. Overactivation of Wnt signaling in NMPs residing in the PS leads to their differentiation into mesoderm progenitors (red) and then further into lateral mesoderm (orange), resulting in abrogated development of body midline structures.

marker Foxa2 (Fig. S8*F*, *Lower*, arrow), affirming their mesodermal identity. Together, these observations demonstrated that the fate of NMPs residing in the PS was skewed toward lateral mesoderm instead of neuroectoderm and paraxial mesoderm.

Together, these results indicated that, in *Tet1/2/3* TKO embryos, anterior patterning was severely disrupted, with deficiencies in head development. In posterior development, NMPs located in the NSB/CLE, which are normally committed to develop into both neural plate and paraxial mesoderm all along the anterior–posterior (AP) body axis, were skewed to a lateral mesodermal cell fate, likely owing to overactivation of Wnt signaling (model in Fig. 6*I*). These in vivo observations are completely consistent with the aberrant differentiation of *Tet3* KO and *Tet1/2/3* TKO ESCs in serum-free conditions in vitro, in which we observed a decrease of neuroectodermal markers and an increase of cardiac mesodermal markers.

Discussion

Here, we show that Tet proteins, especially Tet3, are key transcriptional regulators that maintain the balance between neuroectodermal and mesodermal cell fate determination by repressing Wnt signaling. Both Tet3- and Tet1/2/3-deficient mESCs showed impaired neural conversion, with skewing toward cardiac mesoderm in serum free conditions. Conversely, ectopic *Tet3* expression enhanced neuroectoderm differentiation and limited cardiac mesoderm specification. Impaired neuroectodermal differentiation and increased cardiac mesodermal specification of *Tet3*-deficient mESCs was rescued by addition of the extracellular Wnt inhibitor Dkk1. Our results demonstrate a key role for Tet3 in establishing the correct balance between neural and mesodermal cell fate through modulation of Wnt signaling in mESCs and emphasize a clear functional redundancy between TET-family enzymes in vivo.

Although *Tet3* KO embryos developed until birth and showed no overt cardiac and neuronal phenotypes other than an increase in Isl-1 expression in the right ventricle, *Tet1/2/3*-deficient embryos showed major defects in neural development, manifesting a complete absence of midline structures, including the posterior neural tube, somites, and NC. Differences in single *Tet3* vs. triple *Tet* KOs is most likely due to functional redundancy from the other two Tet family members, *Tet1* and *Tet2*. In WT embryos, NMPs residing in the NSB and CLE contribute to both neural tube and paraxial mesoderm all along the AP body axis (24–27) (Fig. 6 *I*, *Left*). Timing and duration of Wnt activity are important parameters for the induction and maintenance of NMPs, which maintain self-renewal and bipotency at moderate levels of Wnt signaling: Cells exposed to a low-Wnt environment become neural, whereas cells exposed to high levels of Wnt transition to a mesodermal fate (47, 50, 51). Our studies of Tet1/2/3-deficient embryos and Tet3-deficient mESCs indicated that Wnt signaling was abnormally activated in the absence of TET proteins, particularly Tet3. Overactivation of Wnt signaling in NMPs residing in the PS region led to their differentiation into lateral mesoderm at the expense of neuroectoderm and paraxial mesoderm fate, resulting in abrogated development of body midline structures (Fig. 6 *I*, *Right*).

A precedent for this phenotype occurring downstream of hyperactivated Wnt signaling is provided by a transgenic mouse line in which ectopic Wnt3a is driven by a Cdx2 enhancer in the posterior epiblast. In Cdx2P–Wnt3a embryos, neuroectodermal specification is adversely affected, as evidenced by strong down-regulation of Sox2. However, activation of Wnt3a does not result in overproduction of paraxial mesoderm, but, rather, resulted in ectopic lateral mesoderm expressing Wnt2 and Tbx4 (47). Previous studies have demonstrated that specification of lateral mesoderm at the expense of paraxial mesoderm occurs in the absence of signaling from the neural tube, offering an explanation as to why lateral mesodermal fate, rather than paraxial mesodermal fate, is observed with loss of neural specification (49).

Tet1/2/3-deficient embryos also displayed defects in development of ANP. Indeed, formation of anterior neural structures requires suppression of Wnt signals, because mouse embryos deficient for the Wnt antagonist Dkk1 are headless (52). However, defects in ANP development were not fully penetrant and therefore could be secondary: Recent studies point to a role of node derivatives such as the NC and somites in maintaining and stabilizing anterior neural specification (53). In *Hnf3b*/*Foxa2* conditional mutants, which lack paraxial mesoderm, specification of the ANP occurs, but is labile (54).

Besides their functionally redundant roles in the generation of oxi-mC, TET-family members also display distinct roles, in part because they are expressed in different cellular locations or at different developmental stages (18, 32), and regulate oxi-mC levels at different genomic locations (55, 56). Although there is some overlap, Tet1 primarily regulates 5hmC levels at gene promoters and TSSs, whereas Tet2 mainly regulates 5hmC levels in gene bodies (55). Our Tet3 ChIP-seq data in NPCs show that Tet3-binding sites also cluster close to TSSs, with a low frequency of binding at distal regions relative to the TSS, suggesting that Tet1 and Tet3 may have similar functions, despite their distinct temporal expression patterns during mESC differentiation (Fig.1*A*) (32). To gain further insights into the redundant and specific functions of TET proteins during embryogenesis, we will need to develop new techniques that enable genome-wide profiling of distinct cellular lineages, ideally at a single-cell level, in TET-deficient embryos.

A recent publication (57) showed that *Tet1/2/3* TKO embryos display patterning defects in association with impaired specification of paraxial mesoderm. The authors suggested that hyperactive Nodal signaling contributed to the patterning defects in *Tet1/2/3* TKO embryos. Our data extend their findings. We show that overactivation of Wnt signaling in NMPs leads to their differentiation into lateral mesoderm at the expense of neuroectoderm and paraxial mesoderm fate. We also show a strong correlation between the expression levels of Wnt3 and Nodal in both control and *Tet1/2/3* TKO embryos at the gastrulation stage: Expression of both Wnt3 and Nodal RNAs decreased sharply from E7.25 to E7.5 in WT control embryos, but was high in *Tet1/2/3* TKO embryos at day 7.5 (Fig. S8*G*). Notably, Wnt3 was shown to activate Nodal expression directly through its proximal epiblast enhancer at the gastrulation stage (58, 59). Xu and colleagues (57) observed that Wnt3 is strongly expressed in posterior of PS in *Tet1/2/3* TKO embryos at E7.5, where we also found strong signals for the active form of β-catenin (Fig. S8*E*). Therefore, it is likely that Wnt and Nodal signaling pathways are both involved in Tet1/2/3-regulated embryonic patterning processes.

Materials and Methods

Detailed materials and methods are described in *SI Materials and Methods*. Dataset S4 lists the primers used for qRT-PCR, bisulfite sequencing and genotyping.

ACKNOWLEDGMENTS. We thank Dr. Guoliang Xu for generously providing Tet3 antibody; Susan Togher and Ryan Hastie for animal genotyping; the La Jolla Institute sequencing facility for next-generation sequencing; and the La Jolla Institute microscopy and histology facility for help with histological and microscopic analysis. This work was supported by NIH Grants R01 CA151535 and R01 HD065812 (to A.R.). X.L. was supported by CIRM UCSD Interdisciplinary Stem Cell Research & Training Grant II Postdoctoral Fellowship TG2-01154.

1. Tahiliani M, et al. (2009) Conversion of 5-methylcytosine to 5-hydroxymethylcytosine in mammalian DNA by MLL partner TET1. *Science* 324(5929):930–935.
2. Ko M, et al. (2010) Impaired hydroxylation of 5-methylcytosine in myeloid cancers with mutant TET2. *Nature* 468(7325):839–843.
3. Ito S, et al. (2011) Tet proteins can convert 5-methylcytosine to 5-formylcytosine and 5-carboxylcytosine. *Science* 333(6047):1300–1303.
4. Pastor WA, Aravind L, Rao A (2013) TETonic shift: Biological roles of TET proteins in DNA demethylation and transcription. *Nat Rev Mol Cell Biol* 14(6):341–356.

5. Ko M, et al. (2013) Modulation of TET2 expression and 5-methylcytosine oxidation by the CXXC domain protein IDAX. *Nature* 497(7447):122–126.
6. Spruijt CG, et al. (2013) Dynamic readers for 5-(hydroxy)methylcytosine and its oxidized derivatives. *Cell* 152(5):1146–1159.
7. Mellén M, Ayata P, Dewell S, Kriaucionis S, Heintz N (2012) MeCP2 binds to 5hmC enriched within active genes and accessible chromatin in the nervous system. *Cell* 151(7):1417–1430.
8. Hashimoto H, et al. (2014) Wilms tumor protein recognizes 5-carboxylcytosine within a specific DNA sequence. *Genes Dev* 28(20):2304–2313.
9. Tan L, Shi YG (2012) Tet family proteins and 5-hydroxymethylcytosine in development and disease. *Development* 139(11):1895–1902.
10. Dawlaty MM, et al. (2011) Tet1 is dispensable for maintaining pluripotency and its loss is compatible with embryonic and postnatal development. *Cell Stem Cell* 9(2): 166–175.
11. Rudenko A, et al. (2013) Tet1 is critical for neuronal activity-regulated gene expression and memory extinction. *Neuron* 79(6):1109–1122.
12. Zhang RR, et al. (2013) Tet1 regulates adult hippocampal neurogenesis and cognition. *Cell Stem Cell* 13(2):237–245.
13. Cimmino L, et al. (2015) TET1 is a tumor suppressor of hematopoietic malignancy. *Nat Immunol* 16(6):653–662.
14. Ko M, et al. (2011) Ten-Eleven-Translocation 2 (TET2) negatively regulates homeostasis and differentiation of hematopoietic stem cells in mice. *Proc Natl Acad Sci USA* 108(35):14566–14571.
15. Moran-Crusio K, et al. (2011) Tet2 loss leads to increased hematopoietic stem cell self-renewal and myeloid transformation. *Cancer Cell* 20(1):11–24.
16. Gu TP, et al. (2011) The role of Tet3 DNA dioxygenase in epigenetic reprogramming by oocytes. *Nature* 477(7366):606–610.
17. Dawlaty MM, et al. (2013) Combined deficiency of Tet1 and Tet2 causes epigenetic abnormalities but is compatible with postnatal development. *Dev Cell* 24(3):310–323.
18. Kang J, et al. (2015) Simultaneous deletion of the methylcytosine oxidases Tet1 and Tet3 increases transcriptome variability in early embryogenesis. *Proc Natl Acad Sci USA* 112(31):E4236–E4245.
19. Kriaucionis S, Heintz N (2009) The nuclear DNA base 5-hydroxymethylcytosine is present in Purkinje neurons and the brain. *Science* 324(5929):929–930.
20. Szulwach KE, et al. (2011) 5-hmC-mediated epigenetic dynamics during postnatal neurodevelopment and aging. *Nat Neurosci* 14(12):1607–1616.
21. Xu Y, et al. (2012) Tet3 CXXC domain and dioxygenase activity cooperatively regulate key genes for Xenopus eye and neural development. *Cell* 151(6):1200–1213.
22. Copp AJ, Greene ND, Murdoch JN (2003) The genetic basis of mammalian neurulation. *Nat Rev Genet* 4(10):784–793.
23. Iwafuchi-Doi M, et al. (2011) The Pou5f1/Pou3f-dependent but SoxB-independent regulation of conserved enhancer N2 initiates Sox2 expression during epiblast to neural plate stages in vertebrates. *Dev Biol* 352(2):354–366.
24. Henrique D, Abranches E, Verrier L, Storey KG (2015) Neuromesodermal progenitors and the making of the spinal cord. *Development* 142(17):2864–2875.
25. Cambray N, Wilson V (2002) Axial progenitors with extensive potency are localised to the mouse chordoneural hinge. *Development* 129(20):4855–4866.
26. Cambray N, Wilson V (2007) Two distinct sources for a population of maturing axial progenitors. *Development* 134(15):2829–2840.
27. Tzouanacou E, Wegener A, Wymeersch FJ, Wilson V, Nicolas JF (2009) Redefining the progression of lineage segregations during mammalian embryogenesis by clonal analysis. *Dev Cell* 17(3):365–376.
28. Muñoz-Sanjuán I, Brivanlou AH (2002) Neural induction, the default model and embryonic stem cells. *Nat Rev Neurosci* 3(4):271–280.
29. Kamiya D, et al. (2011) Intrinsic transition of embryonic stem-cell differentiation into neural progenitors. *Nature* 470(7335):503–509.
30. Murry CE, Keller G (2008) Differentiation of embryonic stem cells to clinically relevant populations: Lessons from embryonic development. *Cell* 132(4):661–680.
31. Watanabe K, et al. (2005) Directed differentiation of telencephalic precursors from embryonic stem cells. *Nat Neurosci* 8(3):288–296.
32. Koh KP, et al. (2011) Tet1 and Tet2 regulate 5-hydroxymethylcytosine production and cell lineage specification in mouse embryonic stem cells. *Cell Stem Cell* 8(2):200–213.
33. Veeman MT, Slusarski DC, Kaykas A, Louie SH, Moon RT (2003) Zebrafish prickle, a modulator of noncanonical Wnt/Fz signaling, regulates gastrulation movements. *Curr Biol* 13(8):680–685.
34. Semënov MV, et al. (2001) Head inducer Dickkopf-1 is a ligand for Wnt coreceptor LRP6. *Curr Biol* 11(12):951–961.
35. Linhart HG, et al. (2007) Dnmt3b promotes tumorigenesis in vivo by gene-specific de novo methylation and transcriptional silencing. *Genes Dev* 21(23):3110–3122.
36. Suzuki H, et al. (2004) Epigenetic inactivation of SFRP genes allows constitutive WNT signaling in colorectal cancer. *Nat Genet* 36(4):417–422.
37. Huang Y, et al. (2010) The behaviour of 5-hydroxymethylcytosine in bisulfite sequencing. *PLoS One* 5(1):e8888.
38. Toyoda S, et al. (2014) Developmental epigenetic modification regulates stochastic expression of clustered protocadherin genes, generating single neuron diversity. *Neuron* 82(1):94–108.
39. Kawaguchi M, et al. (2008) Relationship between DNA methylation states and transcription of individual isoforms encoded by the protocadherin-alpha gene cluster. *J Biol Chem* 283(18):12064–12075.
40. Dallosso AR, et al. (2009) Frequent long-range epigenetic silencing of protocadherin gene clusters on chromosome 5q31 in Wilms' tumor. *PLoS Genet* 5(11):e1000745.
41. Dallosso AR, et al. (2012) Long-range epigenetic silencing of chromosome 5q31 protocadherins is involved in early and late stages of colorectal tumorigenesis through modulation of oncogenic pathways. *Oncogene* 31(40):4409–4419.
42. Kietzmann A, Wang Y, Weber D, Steinbeisser H (2012) Xenopus paraxial protocadherin inhibits Wnt/β-catenin signalling via casein kinase 2β. *EMBO Rep* 13(2): 129–134.
43. Christov M, Koren S, Yuan Q, Baron R, Lanske B (2011) Genetic ablation of sfrp4 in mice does not affect serum phosphate homeostasis. *Endocrinology* 152(5):2031–2036.
44. Qyang Y, et al. (2007) The renewal and differentiation of Isl1+ cardiovascular progenitors are controlled by a Wnt/beta-catenin pathway. *Cell Stem Cell* 1(2):165–179.
45. Dawlaty MM, et al. (2014) Loss of Tet enzymes compromises proper differentiation of embryonic stem cells. *Dev Cell* 29(1):102–111.
46. Lin HH, et al. (2010) Neuronatin promotes neural lineage in ESCs via Ca(2+) signaling. *Stem Cells* 28(11):1950–1960.
47. Jurberg AD, Aires R, Nóvoa A, Rowland JE, Mallo M (2014) Compartment-dependent activities of Wnt3a/β-catenin signaling during vertebrate axial extension. *Dev Biol* 394(2):253–263.
48. Zaffran S, Frasch M (2002) Early signals in cardiac development. *Circ Res* 91(6): 457–469.
49. Schultheiss TM, Burch JB, Lassar AB (1997) A role for bone morphogenetic proteins in the induction of cardiac myogenesis. *Genes Dev* 11(4):451–462.
50. Martin BL, Kimelman D (2012) Canonical Wnt signaling dynamically controls multiple stem cell fate decisions during vertebrate body formation. *Dev Cell* 22(1):223–232.
51. Bouldin CM, et al. (2015) Wnt signaling and tbx16 form a bistable switch to commit bipotential progenitors to mesoderm. *Development* 142(14):2499–2507.
52. Mukhopadhyay M, et al. (2001) Dickkopf1 is required for embryonic head induction and limb morphogenesis in the mouse. *Dev Cell* 1(3):423–434.
53. Camus A, et al. (2000) The morphogenetic role of midline mesendoderm and ectoderm in the development of the forebrain and the midbrain of the mouse embryo. *Development* 127(9):1799–1813.
54. Hallonet M, et al. (2002) Maintenance of the specification of the anterior definitive endoderm and forebrain depends on the axial mesendoderm: A study using HNF3beta/Foxa2 conditional mutants. *Dev Biol* 243(1):20–33.
55. Huang Y, et al. (2014) Distinct roles of the methylcytosine oxidases Tet1 and Tet2 in mouse embryonic stem cells. *Proc Natl Acad Sci USA* 111(4):1361–1366.
56. Hon GC, et al. (2014) 5mC oxidation by Tet2 modulates enhancer activity and timing of transcriptome reprogramming during differentiation. *Mol Cell* 56(2):286–297.
57. Dai HQ, et al. (2016) TET-mediated DNA demethylation controls gastrulation by regulating Lefty-Nodal signalling. *Nature* 538(7626):528–532.
58. Ben-Haim N, et al. (2006) The nodal precursor acting via activin receptors induces mesoderm by maintaining a source of its convertases and BMP4. *Dev Cell* 11(3): 313–323.
59. Arnold SJ, Robertson EJ (2009) Making a commitment: Cell lineage allocation and axis patterning in the early mouse embryo. *Nat Rev Mol Cell Biol* 10(2):91–103.
60. Chambers I, et al. (2003) Functional expression cloning of Nanog, a pluripotency sustaining factor in embryonic stem cells. *Cell* 113(5):643–655.
61. Li X, et al. (2011) Calcineurin-NFAT signaling critically regulates early lineage specification in mouse embryonic stem cells and embryos. *Cell Stem Cell* 8(1):46–58.
62. Ying QL, Smith AG (2003) Defined conditions for neural commitment and differentiation. *Methods Enzymol* 365:327–341.
63. Lewandoski M, Wassarman KM, Martin GR (1997) Zp3-cre, a transgenic mouse line for the activation or inactivation of loxP-flanked target genes specifically in the female germ line. *Curr Biol* 7(2):148–151.
64. Sadate-Ngatchou PI, Payne CJ, Dearth AT, Braun RE (2008) Cre recombinase activity specific to postnatal, premeiotic male germ cells in transgenic mice. *Genesis* 46(12): 738–742.
65. Lin L, et al. (2007) Beta-catenin directly regulates Islet1 expression in cardiovascular progenitors and is required for multiple aspects of cardiogenesis. *Proc Natl Acad Sci USA* 104(22):9313–9318.
66. Zhang Y, et al. (2008) Model-based analysis of ChIP-Seq (MACS). *Genome Biol* 9(9): R137.
67. Ji X, Li W, Song J, Wei L, Liu XS (2006) CEAS: Cis-regulatory element annotation system. *Nucleic Acids Res* 34(Web Server issue):W551–554.
68. Chen TW, et al. (2014) ChIPseek, a web-based analysis tool for ChIP data. *BMC Genomics* 15:539.
69. Heinz S, et al. (2010) Simple combinations of lineage-determining transcription factors prime cis-regulatory elements required for macrophage and B cell identities. *Mol Cell* 38(4):576–589.
70. Yue X, et al. (2016) Control of Foxp3 stability through modulation of TET activity. *J Exp Med* 213(3):377–397.
71. Guo W, et al. (2013) BS-Seeker2: A versatile aligning pipeline for bisulfite sequencing data. *BMC Genomics* 14:774.